Theoretical derivation of artificially cemented granular soils strength

A. Diambra, PhD, MEng**,** Lecturer**,** Queen's School of Engineering, University of Bristol, Bristol, UK

E. Ibraim, PhD, MEng**,** Reader, Queen's School of Engineering, University of Bristol, Bristol, UK

A. Peccin , MEng**,** Engineering School, Federal University of Rio Grande do Sul, Porto Alegre, Brazil

N. C. Consoli, PhD, MEng**,** Professor, Engineering School, Federal University of Rio Grande do Sul, Porto Alegre, Brazil

L. Festugato, PhD, MEng**,** Lecturer, Engineering School, Federal University of Rio Grande do Sul, Porto Alegre, Brazil

Revised submission for possible publication in:

ASCE Journal of Geotechnical and Geoenvironmental Engineering

17/08/2016

Author to receive correspondence: Dr Andrea Diambra
Lecturer in Geomechanics
Queen's School of Engineering
University of Bristol
Bristol (UK)
andrea.diambra@bristol.ac.uk

Number of words: 4220 approx
Number of figures: 9
Number of tables: 2

ABSTRACT

This paper provides a theoretical derivation for the unconfined compression strength of artificially cemented granular soils. The proposed developments are based on the concept of superposition of failure strength contributions of the soil and cement phases. The granular matrix obeys the critical state soil mechanics concept, while the strength of the cemented phase can be described using the Drucker-Prager failure criterion. In the process, the analytical relation is suitably adjusted to parallel a recently proposed empirical relationship that links unconfined compression strength of artificially cemented granular soils to an adjusted porosity/cement ratio parameter. While the proposed analytical relation fits well the experimental data for different granular soils and cement curing time, further parametric analysis offers the possibility to explore the effect of some material parameters on the unconfined compression strength of artificially cemented granular soils.

Keywords: Portland cement, porosity, granular soils, porosity/cement ratio.

1 INTRODUCTION

Over the last decades, there has been an increasing interest in exploring techniques to artificially improve the mechanical performances of soils in order to meet progressively stricter operational criteria for geotechnical structures. Mixing soils with small amounts of binding agents, such as cement, aims to reproduce the stable internal structure of naturally cemented or weakly bonded soils. Artificial cementation of granular soils results in an increased stiffness and peak strength (e.g. Saxena and Lastrico, 1978; Dupas and Pecker, 1979; Clough et al. 1981) associated with a more dilative response (e.g. Lade and Overton 1989; Schnaid et al. 2001) and a pronounced post-peak brittleness (e,g, Abdulla and Kiousis 1997a;

Wang and Leung, 2008). It also gives rise to some tensile strength (e.g. Leroueil and Vaughan, 1990; Clough et al. 1981). However, laboratory experiments under high confining pressures have shown that the beneficial strength and stiffness contributions of the cementing bonds can be reduced or even suppressed. The cemented bonds can break under the applied stress leaving the frictional resistance of the sand matrix to become again the controlling strength component (Coop and Atkinson, 1993; Rabbi and Kuwano, 2012).

Artificial cementation of granular soils has been successfully applied to control excessive displacement/settlement of shallow foundations, in slope protection for earth dams, to prevent liquefaction of loose granular soils and in pavement base layers (e.g Saxena et al. 1988; Porbaha et al. 1998; Gallagher and Mitchell, 2002; Thomé et al. 2005; Mitrani and Madabhushi 2010). These are geotechnical applications which have in common a low confining stress level. In these situations, composite's strength characterisation from unconfined compression tests may offer relevant results towards an appropriate soil/cement mixture design (e.g. Gomez and Anderson 2012).

The unconfined compressive strength (q_u) of artificially cemented granular soils is positively influenced by an increase in cement content and decrease in porosity (e.g. Clough et al. 1981 and Maccarini 1987). However, it has been recently found by Consoli *et al.* (2007) that an adjusted porosity/cement ratio (η/C_{iv}^{c}) can be plotted against unconfined compressive strength to describe a unique hyperbolic relationship for a given soil and cement type (see Fig. 1a) of the following form:

$$q_u = B\left(\frac{\eta}{{C_{iv}}^{c}}\right)^{b} \quad (1)$$

where porosity (η) is expressed as percentage of the volume of voids divided by total volume of the specimen while volumetric cement content (C_{iv}) is expressed as percentage of the volume of cement divided by the total volume of the specimen. Consoli *et al.* (2009a,b, 2011a,b, 2014a,b and 2015) and Consoli (2014) have successfully shown and confirmed the usefulness of such ratio in controlling strength of several soils and binders. The exponent, c, on the top of C_{iv} is found to be about 1.0 for clean granular soils treated with Portland cement (Consoli *et al.* 2010, 2013) and smaller than unity for granular soils contaminated by fines, silts and/or clays, (Consoli *et al.* 2012) as exemplified in Fig.1a. The particle size distributions for the three analysed materials are also reported in Fig.1b.

Beyond the effect of the properties of the constituents (granular soil matrix and binder), the unconfined compressive strength of artificially cemented granular soils is also affected by other testing variables, such as curing time (e.g. Rabbi and Kuwano, 2012). As shown in Fig.2 (Consoli *et al*. 2013), for each curing period, it is still possible to fit the experimental data with relations of type (1) for fixed c and b and different B values.

A number of theoretical models have been proposed for predicting the overall constitutive behaviour of cemented soils. These are generally based on modifications of state boundary surfaces and hardening rules adopted for granular soils (e.g. Hirai et al., 1989; Sun and Matsuoka, 1999) or they consider the cemented soil as a multiphase material imposing the superposition of the stress contributions of cement bonds and sand grains (e.g. Abdulla and Kiousis 1997b; Vatsala et al. 2001). However, for unconfined compression test conditions, it has been shown that the simple relationship proposed in Eq. (1) can successfully predict the strength of a broad range of cemented soils using only three model parameters. Nevertheless, the empirical nature of its derivation has not permitted to establish meaningful connections

between its governing coefficients and relevant material properties. In contrast, this paper approaches the problem of artificially cemented soil from a different perspective by proposing an analytical relationship for the unconfined compression strength based on the superposition of failure strength contributions of the individual constituents: soil matrix and cement. Insight into the physical meaning of governing coefficients for the unconfined compression strength unconfined compression strength is gained by conveniently adjusting the analytically derived relationship to parallel the empirical hyperbolic relationship (1). Finally, a parametric analysis exploring the effect of some material parameters on the unconfined compression strength of cemented soils is conducted.

2 THEORETICAL MODEL

The artificially cemented soil composite material is composed by the soil phase (the granular matrix) and the cement phase. It is assumed that:

1) The composite cemented material is isotropic.

2) The behaviour of the cemented soil at the failure point is determined by superposing the strength contributions of both phases (similarly to stress superposition approach used by Abdulla and Kiousis 1997b; Vatsala et al., 2001).

3) The failure of the composite cemented material occurs as a result of a simultaneous failure of both the cemented and the soil matrix phases.

4) Strain compatibility between the composite and its two phases, soil and cement, applies (similarly to the parallel spring approach assumed in Vatsala et al., 2001).

By using a volumetric averaging approach (Diambra et al., 2011; Diambra et al., 2013; Diambra and Ibraim 2015), the failure stress state of the composite (**σ**) can be derived from the failure stresses of its constituents ($\boldsymbol{\sigma}_{\mathbf{m}}$ and $\boldsymbol{\sigma}_{\mathbf{c}}$ for the sand matrix and cement phase, respectively) by the following relationship:

$$\boldsymbol{\sigma} = \mu_m \boldsymbol{\sigma}_{\mathbf{m}} + \mu_c \boldsymbol{\sigma}_{\mathbf{c}} \quad (2)$$

where μ_m and μ_c are the volumetric concentrations of soil and cement in the composite material, respectively. It should be noted that the volumetric cement concentration μ_c equals C_{iv}/100. The relation (2) can be expanded in the terms of total mean (p) and deviatoric (q) stress components to satisfy the axisymmetric stress conditions of an unconfined compression test:

$$\begin{bmatrix} q \\ p \end{bmatrix} = \mu_m \begin{bmatrix} q_m \\ p_m \end{bmatrix} + \mu_c \begin{bmatrix} q_c \\ p_c \end{bmatrix} \quad (3)$$

It is now necessary to define the stress failure conditions for the two phases.

Failure for the cement phase

It is considered that the strength of the cement phase is described by the Drucker-Prager failure criterion, which can be expressed in terms of the deviatoric and isotropic stresses as follows:

$$q_c = c_c + M_c p_c \quad (4)$$

where the terms c_c and M_c can be linked to both the uniaxial compressive, σ_c^c, and tensile, σ_c^t, strengths of the cement binder by the following expressions:

$$c_c = 2\frac{\sigma_c^c}{1-\beta} \quad (5)$$

and

$$M_c = 3\frac{\beta+1}{\beta-1} \quad (6)$$

where β represents the ratio between the uniaxial compression and extension strengths:

$$\beta = \frac{\sigma_c^c}{\sigma_c^t} \quad (7)$$

Failure for the soil phase

The strength of granular soils is generally represented using the density dependent deviatoric stress and mean stress ratio, (q_m/p_m). In soil constitutive modelling, it is customary to link the strength of the material with a state parameter (ψ), which quantifies the difference between the current density state from the corresponding one at critical state (Been and Jefferies, 1985). For the following modelling development, it is simpler to define the state parameter in terms of the material porosity (η for current porosity and η_{cs} for the corresponding porosity at the critical state) using the following definition:

$$\psi = \frac{\eta_{cs}}{\eta} \quad (8)$$

where ψ>1 represents a state on the loose side of the critical state line (CSL), while ψ<1 represents a state on the dense side of the CSL.

The granular soil stress ratio at failure can then be expressed by the following expression:

$$\frac{q_m}{p_m} = M^* = M\left(\frac{\eta_{cs}}{\eta}\right)^a \quad (9)$$

where M^* is the peak strength, M is the critical state strength and a is a model parameter which links the peak strength to the state parameter, ψ. It is also assumed that grain crushing,

159 which may affect the strength of the soil matrix and the overall failure mode of cemented
160 sands (Leroueil and Vaughan, 1990), does not occur during loading.

161 **Strength relationship for artificially cemented soil**

162 By substituting (4) and (9) into equation (3), the following expression for the unconfined
163 compressive strength (q_u) is derived:

164 $$q_u = 3\mu_c \left(\frac{c_c + M_c p_c - M^* p_c}{3 - M^*}\right) \quad (10)$$

165 In order to have a relationship based solely on cement and soil phase strengths, an estimation
166 of the confining stress of the cement phase, p_c, is required. It appears reasonable first to
167 assume that, under unconfined compression test conditions, the cemented soils exhibit a
168 quasi-elastic behaviour up to the peak strength conditions (Consoli *et al*., 2009a). Thus, the
169 following relationship between radial (ε_r) and axial (ε_a) composite strains can be considered:

170 $$\varepsilon_r = -\nu\, \varepsilon_a \quad (11)$$

171 where ν is the cemented soil composite Poisson's ratio. Based on the strain compatibility
172 assumption, the cement phase is subjected to the same strain field and, assuming similarly
173 an elastic behaviour, it is possible to derive the ratio K_c between the cement deviatoric and
174 isotropic stresses, q_c and p_c respectively:

175 $$\frac{q_c}{p_c} = K_c = 3\frac{1+\nu}{1+\nu_c}\frac{1-2\nu_c}{1-2\nu} \quad (12)$$

176 where ν_c is the cement Poisson's ratio. Combination of (4) and (12) provides the following
177 expression for the isotropic stress at failure of the cement phase:

178 $$p_c = \frac{c_c}{K_c - M_c} \quad (13)$$

179 which can also be expressed in terms of the compression strength and the uniaxial stress ratio
180 by substituting (5) and (6). Further substitution of (13) into (10) leads to the following
181 relationship for the unconfined compression strength:

182 $$q_u = \frac{6\mu_c \sigma_c^c}{K_c(1-\beta)+3(\beta+1)} \left(\frac{K_c - M\left(\frac{\eta_{cs}}{\eta}\right)^a}{3 - M\left(\frac{\eta_{cs}}{\eta}\right)^a} \right) \quad (14)$$

183 As can be observed, (14) provides a direct expression of the unconfined strength of the
184 cemented soil as function of the porosity (η) and the cement content (μ_c) variables, with μ_c
185 =C_{iv}/100, while the parameters are constants relative to both the soil and cement phases, as
186 summarised in Table 1. It should be noted that in this development, which refers to
187 unconfined compression conditions only, the value of the soil porosity at the critical state is
188 considered as a soil constant independent of the mean effective stress.

189 # 3 MODEL PREDICTIONS

190 The validity of the unconfined compression strength expression proposed by (14) is assessed
191 here by direct comparison with experimental data provided by unconfined compression test
192 results performed on three different artificially cemented sands which have been cured for
193 different time periods. The three selected granular matrices, whose particle size distribution
194 is given in Fig. 1b, are quartz-feldspar rich sands which are not expected to crush under typical
195 foundation loading. The simulation exercise has been performed for the following conditions:

196 1) Uniform Osorio sand + early strength Portland cement cured at 2, 7 and 28 days (Consoli
197 *et al*. 2013);

198 2) Well-graded Porto silty sand + early strength Portland cement (Consoli *et al*. 2012); and

199 3) Botucatu residual soil + early strength Portland cement (Consoli *et al*. 2007).

200 ### 3.1.1 Calibration of model parameters

201 As shown in Table 1, the model requires the calibration of six parameters, three for the soil
202 matrix and three for the cement phase. The values of the constants relative to the sand matrix
203 have been selected based on triaxial experimental results and the assumed values are also
204 indicated in Table 1. The values of critical state strength ratio, *M* (linked to the critical state
205 friction angle φ), for Osorio sand, Botucatu residual soil and Porto silty sand have been
206 derived from Dos Santos *et al*. (2010), Ferreira and Bica (2006) and Rios *et al*. (2012),
207 respectively. Based on the same published results, the specific values of the porosity at the
208 critical state (η_{cs}) have been derived from the critical states line defined in the specific volume
209 - mean effective stress plane (υ-*ln* p').

210 The estimation of the parameter *a* for both Osorio sand and Botucatu residual soil required
211 some careful inspection of a set of published triaxial tests by Dos Santos et al. (2010), and
212 Schnaid et al. (2001), respectively and was based on a calibration exercise between data
213 provided by (9) and the peak strength observed in the triaxial tests, as shown in Fig. 3. Values
214 of a = 1.3 for Osorio sand and a = 3.5 for Botucatu residual soil were found.

215 Owing to the lack of available triaxial data for the Porto silty sand, a value of a = 4, in line with
216 the value selected for the Botucatu soil, has been selected considering that both soils present
217 similar particle size distributions (Fig. 2).

218 The value of the model's parameter, β, relative to the cement phase has been selected based
219 on typical ranges of the uniaxial compression and extension cement strength values for the
220 Portland cement (Table 1). Following (12), the value of the parameter K_c is dependent on the

221 Poisson's ratios of the cemented soil material and the cement phase. Extensive experimental
222 characterisation of the elastic properties of cemented soils by Felt and Abram (1957) suggests
223 values of the Poisson's ratio for cemented sand and silts between 0.22 and 0.31 with a median
224 value of about 0.26, while typical values of Poisson's ratio for mortar matrix are around 0.2,
225 as suggested by Narayam Swamy (1971). These lead to a value of $K_c \approx 4$, which is assumed for
226 all three tested soils. Imposing all the values of the parameters above, the strength of the
227 cementing phase, σ_c^c, was determined by matching the unconfined compression strength
228 given by relation (14) with the experimental results. For each material the calibration process
229 used three randomly selected unconfined compression test results. A curve fitting procedure
230 was also employed by Abdulla and Kiousis (1997b) and Vatsala et al. (2001) to calibrate the
231 strength of the cementing bonds. Like in this work, the former authors used unconfined
232 compression strength results but, for the sake of simplicity, a negligible frictional contribution
233 of the sand matrix was assumed. Instead, Vatsala et al. (2001) based their calibration on tests
234 performed at very low confining pressure to maximise the relative bonds' strength
235 contribution. The strengths σ_c^c values for the Botucatu sand and the Porto silty soil (Table 1)
236 are larger than that for the Osorio sand because of the better grading and larger proportion
237 of fines for the former soils.

238 ### 3.1.2 Simulations

239 A direct comparison between model predictions of the unconfined compression strength (q_u)
240 using the parameter listed in Table 1 and the results from the laboratory tests versus the η/C_{iv}
241 ratio is shown in Fig. 4 for the three different types of cemented soils (different densities and
242 cement contents) cured for 7 days.

243 The model predicts reasonably well the unconfined compression strength including the
244 hyperbolic relationship between the two variables. For the Porto silty sand (Fig. 4b) the

experimental data do not converge in a unique curve (Rios et al., 2012) and the model captures this experimental observation too. Moreover, the Porto silty sand cemented material shows a considerably larger strength than the others which equally the model automatically predicts. This is due to both the larger cement strength σ_c^c if compared with the Osorio sand and the values of the parameters assumed for the soil matrix if compared with the Botucatu soil. Ismail et al. (2002a) pointed out that the properties of the soil grains, size and shape, have also a primary influence on the strength of the cemented soil, which is increased by decreasing the particle size and by using round or non-angular soil grains. These soil features are all included in the parameters M, α, η_{cs} of the matrix which are indeed primarily governed by the shape and size distribution of the grains.

The effect of curing time on the unconfined compressive strength of the cemented soil is shown in Fig. 5, where additional experimental results for cemented Osorio sand at 2 and 28 curing periods are compared with the model prediction. As suggested by Rabbi and Kuwano (2012) , the curing time dependency on the overall strength can be captured by assuming an increase of the compressive strength of the cement phase. In these simulations, σ_c^c varies from 30 MPa, to 50 MPa and 70 MPa for 2, 7 and 28 curing days, respectively.

4 DISCUSSION

4.1.1 Parallelism with empirical formula

The proposed relationship (14) based on theoretical considerations has a different form compared with the empirically based relation (1) proposed by Consoli *et al*. (2007). However, the trends in Figures 1, 2, 4 and 5, show that both approaches fit well the experimental data. In order to make a parallelism between the two relationships, relationship (14) should be

further expressed as a linear function of the peak strength of the soil M^* ($M^*=M(\eta_{cs}/\eta)^a$) and this can be achieved by introducing the following approximation:

$$\frac{K_c-M*}{3-M^*} \cong M^*(-0.6+0.45K_c) \quad (15)$$

The use of (15) in to (14) yields to the following expression for the unconfined compression strength:

$$q_u = \frac{6\,M\,\sigma_c^c\,(-0.6+0.45K_c){\eta_{cs}}^a}{100\,\left(K_c(1-\beta)+3(\beta+1)\right)}\left(\frac{C_{iv}}{\eta^a}\right) \quad (16)$$

A full parallelism with the empirical formula (1) proposed by Consoli *et al*. (2007, 2010, 2012) can be completed if (16) is further manipulated to be expressed in the following form:

$$q_u = \frac{6M\,\sigma_c^c\,(-0.6+0.45K_c){\eta_{cs}}^a}{100\,\left(K_c(1-\beta)+3(\beta+1)\right)}\left(\frac{\eta}{{C_{iv}}^{\frac{1}{a}}}\right)^{-a} = B\left(\frac{\eta}{{C_{iv}}^{\frac{1}{a}}}\right)^{-a} \quad (17)$$

where

$$B = \frac{6M\,\sigma_c^c\,(-0.6+0.45K_c){\eta_{cs}}^a}{100\,\left(K_c(1-\beta)+3(\beta+1)\right)} \quad (18)$$

As shown in Fig. 6, the transformation introduced by (15) appears to have a limited effect on the model predictions Following the suggestion by Consoli *et al*. (2007), the horizontal axis is now expressed using the adjusted porosity/cement ratio (η/C_{iv}^c), where the exponent has been imposed equal to $1/a$ following (17). It can be noticed that the imposed transformation of the horizontal axis leads both the experimental data and the model prediction for a given soil to collapse in an almost unique line.

A closer observation of Equations (17) and (18) can now offer some insight on the meaning and the factors governing the parameters introduced by the empirical relation (1):

1) The proposed formulation in (17) suggests that the exponent *b* and *c* in (1) are dependent on the soil matrix related parameter *a*, with *c=1/a*, and *b=-a*. This corroborates well the experimental findings by Consoli *et al*. (2007) who suggested a dependency of *c* coefficient on the grading of the soil matrix.
2) It follows that a rather straightforward relationship *b=-1/c* can be obtained. This is confirmed by the data plotted in Fig. 1 with *b*=-1.5≈-1=-1/c and c=1 for Osorio sand, *b*=-3.4≈-3.57=-1/c and c=0.28 for Botucatu residual soil, and *b*=-4.2≈-4.77=-1/c with c=0.21 for Porto silty sand.
3) Analysis of (18) suggests that the multiplying parameter *B* in (1) is the result of combined properties of the sand matrix and cement phase. The key governing parameters seem to be the frictional strength of the matrix (*M*), and the strength of the cemented phase, σ_c^c.
4) The multiplying factor *B* is also controlled by the value of the exponent *a*, which is controlled by the sand matrix properties. Analysis of the values given by Consoli *et al*. (2007, 2012, 2013) (Fig.1) demonstrates that large values of the exponent *a* lead to higher values of *B,* as suggested by relationship (18).

4.1.2 Parametric analysis

A parametric analysis to investigate the relative importance of the constituents' parameters is performed. The effect of the variation of the cement phase parameters - compressive strength, σ_c^c, between 10 and 500MPa, cement strength ratio, β, from -4 to -8, and cement stress ratio, K_c, between 3.2 and 6 – on the unconfined compression strength is provided in Fig. 7 a-b-c. The basic values of the soil parameters used in this exercise are as follows: σ_c^c= 50 MPa, β=-6, K_c =4, *M*=1.3, η_{cs}=0.35 and *a*=3. By comparing these three plots, it is rather clear that the strength of the cement binder is by far the leading parameter, corroborating the

experimental results of Maccarini (1987), Ismail et al. (2002b) and Haeri et al. (2006).The Poisson's ratio, and the uniaxial strength ratio have a limited influence. The partial effect of the cement stress ratio K_c suggests that the necessary modelling assumption on the deformation behaviour of the cemented soil imposed in (12) has little effect on the final model predictions, thus increasing the confidence on the proposed developments.

The further influence on the predictions of the three model parameters related to the sand matrix are shown in Fig. 7d-e-f. It is clear that the matrix strength ratio M (or friction angle φ) has some effect but much more limited if compared to the strength properties of the cement phase. However, much more caution should be paid particularly to the effects of the critical state porosity and strength porosity dependency as both parameters have some connection with the adjusted porosity-cement ratio variable. Fig. 7e suggests that materials with larger critical state porosity η_{cs} have larger unconfined strength for the same η/C_{iv} ratio and this would rather be misleading considering that these materials will be characterised by larger value of porosities (thus a larger value of η/C_{iv} ratios) for the same relative density. However, a faster decrease of the unconfined compressive strength (q_u) with increasing η/C_{iv} ratio can be observed for larger values of η_{cs}. Analysis of the trends in Fig. 7f must be carried out with similar caution. While it appears that increasing values of a would lead to a rightward shift of the hyperbolic curve, it must be remembered that the horizontal axis is also affected by the assumed value of a. While a direct conclusion cannot be drawn, the analysis of the three soils considered in this study suggests that large values of a are related to soils with larger fine content, which also show a larger unconfined compressive strength as experimentally observed by Ismail et al. (2002a).

From the whole parametric analysis, it clearly appears that the information on the soil matrix mechanical behaviour embedded in the parameters M, α, η_{cs} and a number of three unconfined compression test results to calibrate the value of the cement bond strength , σ_c^c may be sufficient to provide satisfactory predictions of the cemented soil strength over a large spectrum of cement contents and porosities.

4.1.3 Further applicability of the proposed model

The proposed theoretical model has been primary developed for artificially cemented soils, stabilised with Portland cement and fabricated in controlled laboratory conditions. Application to different cement types can be carried out by assuming different values for the cementation bonding parameters. Nevertheless., it must be considered that different binders such as calcite or gypsum, may also affect some macroscopic behavioural features leading to prior and more brittle yielding (Ismail et al., 2002b). This may contradict some of the model assumptions such as the simultaneous failures of the composite constituents.

The proposed model could also be used to predict the unconfined compressive strength of naturally bonded soils. Nevertheless, such assessment should account for the inhomogeneity and variability generally associated with soils formed in a natural environment. As suggested by Abdulla and Kiousis (1997b), further difficulties may arise from the estimation of the exact percentage of cementation. However, this variable may be combined with the strength of the cemented bonds to be considered as an unique model parameter. Further challenges may arise from the presence of anisotropic cementation, arising from the soil formation process, which may lead to anisotropic failure conditions as experimentally observed by Anagnostopoulos et al. (1991) and Coop and Atkinson (1993) or as considered in the theoretical model by Gao and Zhao (2012). Further modifications of the model describing the

strength of the soil matrix may also be necessary for the perspective application to crushable calcareous soil matrices. CONCLUSIONS

A theoretical derivation for the unconfined compression strength of artificially cemented granular soils based on the concept of superposition of failure strength contributions of the soil and cement phases was proposed. Comparison with experimental data and with empirical relations relating the unconfined compression test to the porosity/cement ratio were conducted. The following conclusions can be drawn:

- The use of the superposition of strength contributions of the soil and cement phase, critical state and dependence of shear strength on the state parameter concepts permitted the elaboration of the theoretical framework;
- The theoretical model developed herein satisfactorily simulates experimental data that related q_u of artificially cemented granular soils and η/C_{iv}^c, capturing the effects of material density, bonding and curing periods.
- The convenient adjustment of the theoretical formulation developed herein to parallel a widely used empirical hyperbolic relationship between the unconfined compressive strength (q_u) of cemented soil with an adjusted porosity/cement ratio (η/C_{iv}^c) has shed some light on both the significance and material properties governing the parameters of the empirical relationship; as expected, the compressive strength of the cement binder is by far the key leading parameter in controlling the unconfined compression strength of the cemented soils. This appears dependent to the particle size distribution of the soil matrix. The ratio of the compression/extension uniaxial cement strengths and the strength of the soil matrix have also a visible influence but indeed much less important than the cement matrix strength.

- The proposed theoretical framework, based on calibration of three parameters relative to the soil matrix and three unconfined compression tests results for the strength of the cemented bonds (the two remaining model parameters of the cemented bonds have a limited influence on the model outcomes), enables the prediction of the unconfined compressive strength of cemented soils over a large spectrum of cement contents and porosities. Development of such relationship can offer significant guidance towards the design of specific soil/cement mixture design to satisfy required strength criteria.
- Extension of the proposed model to different types of cement and natural soils could be pursued but considerations on occurrence of grain crushing (especially for calcareous soils), anisotropy of soil fabric and cementation, inhomogeneity of material properties and precise assessment of the exact percentage of cementation among others, should be introduced.

Acknowledgments

The authors gratefully acknowledge the support provided by the UK Royal Academy of Engineering under the Newton Research Collaboration Programme, (Grant reference: NRCP1415/2/2).

References

Abdulla, A. A., and Kiousis, P. D. (1997a). "Behavior of cemented sands—I. Testing." *International Journal for Numerical and Analytical Methods in Geomechanics*, *21*(8), 533-547.

398 Abdulla, A. A., and Kiousis, P. D. (1997b). “Behavior of cemented sands—II.
399 Modelling.” *International Journal for Numerical and Analytical Methods in Geomechanics*, *21*(8),
400 549-568.

401 Anagnostopoulos, A. G., Kalteziotis, N., Tsiambaos, G. K., and Kavvadas, M. (1991). “Geotechnical
402 properties of the Corinth Canal marls.” *Geotechnical and Geological Engineering*, *9*(1), 1-26

403 Been, K. and Jefferies, M.G. (1985). "A state parameter for sands." *Géotechnique* 35(2), 99-112.

404 Clough, G. W., Sitar, N., Bachus, R. C., and Rad, N. S. (1981). “Cemented sands under static
405 loading.” *Journal of Geotechnical Engineering Division*, *107*(6), 799-817.

406 Consoli, N.C. (2014). “A method proposed for the assessment of failure envelopes of cemented
407 sandy soils”. *Engineering Geology*, 169, 61-68.

408 Consoli, N.C.; Foppa, D.; Festugato, L. and Heineck, K.S. (2007). “Key parameters for strength
409 control of artificially cemented soils”. *Journal of Geotechnical and Geoenvironmental*
410 *Engineering*, 133, 197-205.

411 Consoli, N.C.; Viana da Fonseca, A.; Cruz, R.C. and Heineck, K.S. (2009a). “Fundamental parameters
412 for the stiffness and strength control of artificially cemented sand”. *Journal of Geotechnical and*
413 *Geoenvironmental Engineering*, 135, 1347-1353.

414 Consoli, N.C.; Lopes Junior, L.S. and Heineck, K.S. (2009b). “Key parameters for the strength
415 control of lime stabilized soils”. *Journal of Materials in Civil Engineering*, 21, 210-216.

416 Consoli, N.C.; Cruz, R.C.; Floss, M.F. and Festugato, L. (2010). “Parameters controlling tensile and
417 compressive strength of artificially cemented sand”. *Journal of Geotechnical and*
418 *Geoenvironmental Engineering*, 136, 759-763.

419 Consoli, N.C.; Cruz, R.C. and Floss, M.F. (2011a). “Variables controlling strength of artificially
420 cemented sand: Influence of curing time”. *Journal of Materials in Civil Engineering*, 23, 692-696.

421 Consoli, N.C.; Viana da Fonseca, A.; Cruz, R.C. and Silva, S.R. (2011b). "Voids/cement ratio
422 controlling tensile strength of cement treated soils". *Journal of Geotechnical and*
423 *Geoenvironmental Engineering*, 137, 1125-1131.

424 Consoli, N.C.; Viana da Fonseca, A.; Cruz, R.C.; Silva, S.R. and Fonini, A. (2012). "Parameters
425 controlling stiffness and strength of artificially cemented soils". *Géotechnique*, 62, 177-183.

426 Consoli, N.C.; Festugato, L.; Rocha, C.G.; Cruz, R.C. (2013). "Key parameters for strength control of
427 rammed sand-cement mixtures: Influence of types of Portland cement". *Construction and*
428 *Building Materials*, 49, 591-597.

429 Consoli, N.C.; Lopes Junior, L.S.; Consoli, B.S. and Festugato, L. (2014a). "Mohr-Coulomb failure
430 envelopes of lime-treated soils". *Géotechnique*, 64, 165-170.

431 Consoli, N.C.; Rocha, C.G. and Saldanha, R.B. (2014b). "Coal fly ash-carbide lime bricks: An
432 environment friendly building product". *Construction and Building Materials*, 69, 301-309.

433 Consoli, N.C.; Festugato, L.; Consoli, B.S. and Lopes Junior, L.S. (2015). "Assessing failure envelopes
434 of soil fly ash lime blends". *Journal of Materials in Civil Engineering*, 26, 04014174-1 -
435 04014174-8.

436 Coop, M. R., and Atkinson, J. H. (1993). "The mechanics of cemented carbonate
437 sands." *Géotechnique*, *43*(1), 53-67.

438 Diambra, A., Ibraim, E. Russell, A.R. and Muir Wood, D. (2011): "Modelling the undrained
439 response of fibre reinforced sands." *Soils and Foundations* 51(4), 625-636.

440 Diambra, A., Ibraim, E. Russell, A.R. and Muir Wood, D. (2013) "Fibre reinforced sands: from
441 experiments to modelling and beyond." *International Journal for Numerical and Analytical*
442 *Methods in Geomechanics,* 37(15), 2427-2455.

443 Diambra, A. and Ibraim, E. (2015) "Fibre-reinforced sand: interaction at the fibre and grain
444 scale." *Géotechnique,* 65(4), 296-308.

445 Dos Santos, A.P.S., Consoli, N.C. and Baudet, B.A. (2010). "The mechanics of fibre-reinforced
446 sand." *Géotechnique,* 60(10), 791-799.

447 Dupas, J. M., and Pecker, A. (1979). "Static and dynamic properties of sand-cement." *Journal of the*
448 *Geotechnical Engineering Division*, *105*(3), 419-436.

449 Felt, E. J., and Abrams, M. S. (1957). Strength and elastic properties of compacted soil-cement
450 mixtures. Am Soc Testing and Matls Spec Tech Publ Portland Cement Assoc R and D Lab Bull.

451 Ferreira, P.M.V. and Bica, A.V.D. (2006). "Problems in identifying the effects of structure and
452 critical state in a soil with a transitional behaviour." *Géotechnique*, 56(7), 445-454.

453 Gallagher, P. M., and Mitchell, J. K. (2002). "Influence of colloidal silica grout on liquefaction
454 potential and cyclic undrained behavior of loose sand." *Soil Dynamics and Earthquake*
455 *Engineering*, *22*(9), 1017-1026.

456 Gao, Z., and Zhao, J. (2012). "Constitutive modeling of artificially cemented sand by considering
457 fabric anisotropy." *Computers and Geotechnics*, *41*, 57-69.

458 Gomez, N.S., and Anderson, D.N. (2012). "Soil cement stabilization - mix design, control and
459 results during construction." ISSMGE - TC 211 International Symposium on Ground
460 Improvement IS-GI Brussels 31 May - 1 June 2012,

461 Haeri, S. M., Hamidi, A., Hosseini, S. M., Asghari, E., and Toll, D. G. (2006). "Effect of cement type on
462 the mechanical behavior of a gravely sand." *Geotechnical and Geological Engineering*, *24*(2),
463 335-360.

464 Hirai, H., Takahashi, M., and Yamada. M. (1989). "An elastic-plastic constitutive model for the
465 behavior of improved sandy soils." *Soils and Foundations 29*(2), 69-84.

466 Ismail, M. A., Joer, H. A., Randolph, M. F., and Meritt, A. (2002a). "Cementation of porous materials
467 using calcite." *Geotechnique*, *52*(5), 313-324.

Ismail, M. A., Joer, H. A., Sim, W. H., and Randolph, M. F. (2002b). "Effect of cement type on shear behavior of cemented calcareous soil." *Journal of Geotechnical and Geoenvironmental Engineering*, *128*(6), 520-529.

Lade, P. V., and Overton, D. D. (1989). "Cementation effects in frictional materials." *Journal of Geotechnical Engineering*, *115*(10), 1373-1387.

Leroueil, S., and Vaughan, P. R. (1990). "The general and congruent effects of structure in natural soils and weak rocks." *Géotechnique*, *40*(3), 467-488.

Maccarini, M. (1987). "Laboratory studies of weakly bonded artificial soil." PhD thesis, University of London.

Mitrani, H., and Madabhushi, S. G. (2010). "Cementation liquefaction remediation for existing buildings." *Proceedings of the Institution of Civil Engineers-Ground Improvement*, *163*(2), 81-94.

Porbaha, A., Tanaka, H., and Kobayashi, M. 1998. "State of the art in deep mixing technology. Part II: Applications." *Ground Improvement*, J. ISSMGE, 22, 125–139.

Rabbi, A. T. M. Z., and Kuwano, J. (2012). "Effect of Curing Time and Confining Pressure on the Mechanical Properties of Cement-Treated Sand." In *GeoCongress 2012: State of the Art and Practice in Geotechnical Engineering,* 996-1005, ASCE.

Rios, S., Viana da Fonseca, A. and Baudet, B.A. (2012). "Effect of the porosity/cement ratio on the compression of cemented soil." *Journal of Geotechnical and Geoenvironmental Engineering,* 138(11), 1422-1426.

Saxena, S. K., and Lastrico, R. M. (1978). "Static properties of lightly cemented sand." *Journal of Geotechnical Engineering Division*, 104(GT12), 1449-1464.

Saxena, S. K., Reddy, K. R., and Avramidis, A. S. (1988). "Liquefaction resistance of artificially cemented sand." *Journal of Geotechnical Engineering*, 114(12), 1395-1413.

Schnaid, F., Prietto, P.D.M. and Consoli, N.C. (2001). "Characterization of cemented sand in triaxial compression." *Journal of Geotechnical and Geoenvironmental Engineering,* 127(10), 857-868.

Sun, D. A., and Matsuoka, H. (1999). "An elastoplastic model for frictional and cohesive materials and its application to cemented sands." *Mechanics of Cohesive-frictional Materials*, *4*(6), 525-543.

Swamy, R. N. (1971). Dynamic Poisson's ratio of Portland cement paste, mortar and concrete. Cement and Concrete Research, 1(5), 559-583.Thomé, A., Donato, M., Consoli, N. C., and Graham, J. (2005). Circular footings on a cemented layer above weak foundation soil. *Canadian Geotechnical Journal*, 42(6), 1569-1584.

Vatsala, A., Nova, R., and Murthy, B. S. (2001). Elastoplastic model for cemented soils. ASCE *Journal of Geotechnical and Geoenvironmental Engineering*, *127*(8), 679-687.

Wang, Y. H. and Leung, S. C. (2008). Characterization of cemented sand by experimental and numerical investigations. *Journal of Geotechnical and Geoenvironmental Engineering*, 134(7), 992-1004

Notation list

	a	Parameter linking peak strength to state parameter
	B	Multiplying parameter in Empirical relationship (1)
	b	Exponent of empirical relationship (1)
	c	Exponent of empirical relationship (1)
	c_c	Cohesion of the cement phase
	C_{iv}	Volumetric cement content (expressed in percentage)
	M	Critical state strength ratio for the soil

514	M_c	Slope of the failure line for the cement phase in the q_c -p_c plane
515	M^*	Peak strength ratio for the soil
516	K_c	Cement stress ratio
517	p	Mean stress of the cemented soil
518	p_c	Mean stress of the cement phase
519	p_m	Mean stress of the soil matrix
520	q	Deviator stress of the cement soil
521	q_c	Deviator stress of the cement phase
522	q_m	Deviator stress of the soil matrix
523	q_u	Unconfined compressive strength for the cemented soil
524	β	Ratio between the uniaxial compression and extension strengths
525	φ	Friction angle for the soil matrix
526	ε_a	Axial strain for cemented soil
527	ε_r	Radial strain for cemented soil
528	ν	Poisson's ratio for cemented soil
529	ν_c	Poisson's ratio for cement phase
530	μ_c	Volumetric cement concentration
531	μ_m	Volumetric soil matrix concentration
532	ψ	State parameter
533	η	Porosity
534	η_{cs}	Porosity at critical state
535	σ_c^c	Uniaxial compressive strength of the cement
536	σ_c^t	Uniaxial tensile strength of the cement
537		

Table 1. Parameters of the proposed model

Symbol	Variable	Values		
		Osorio sand	**Porto silty sand**	**Botucatu residual soil**
M	Critical state soil strength ratio	1.33 (φ≈33°)	1.35 (φ≈33.5°)	1.25 (φ≈31.5°)
η_{cs}	Critical state soil porosity	44	36	30
a	Parameter governing dependence of soil strength on its density	1.3	4	3.5
σ_c^c	Cement phase compressive strength	30 MPa (2 days during) 50 MPa (7 days curing) 70 (28 days curing)	90 MPa (7 days curing)	90 MPa (7 days curing)
β	Uniaxial compression and extension cement strength ratio	-6	-6	-6
K_c	Cement stress ratio	4	4	4

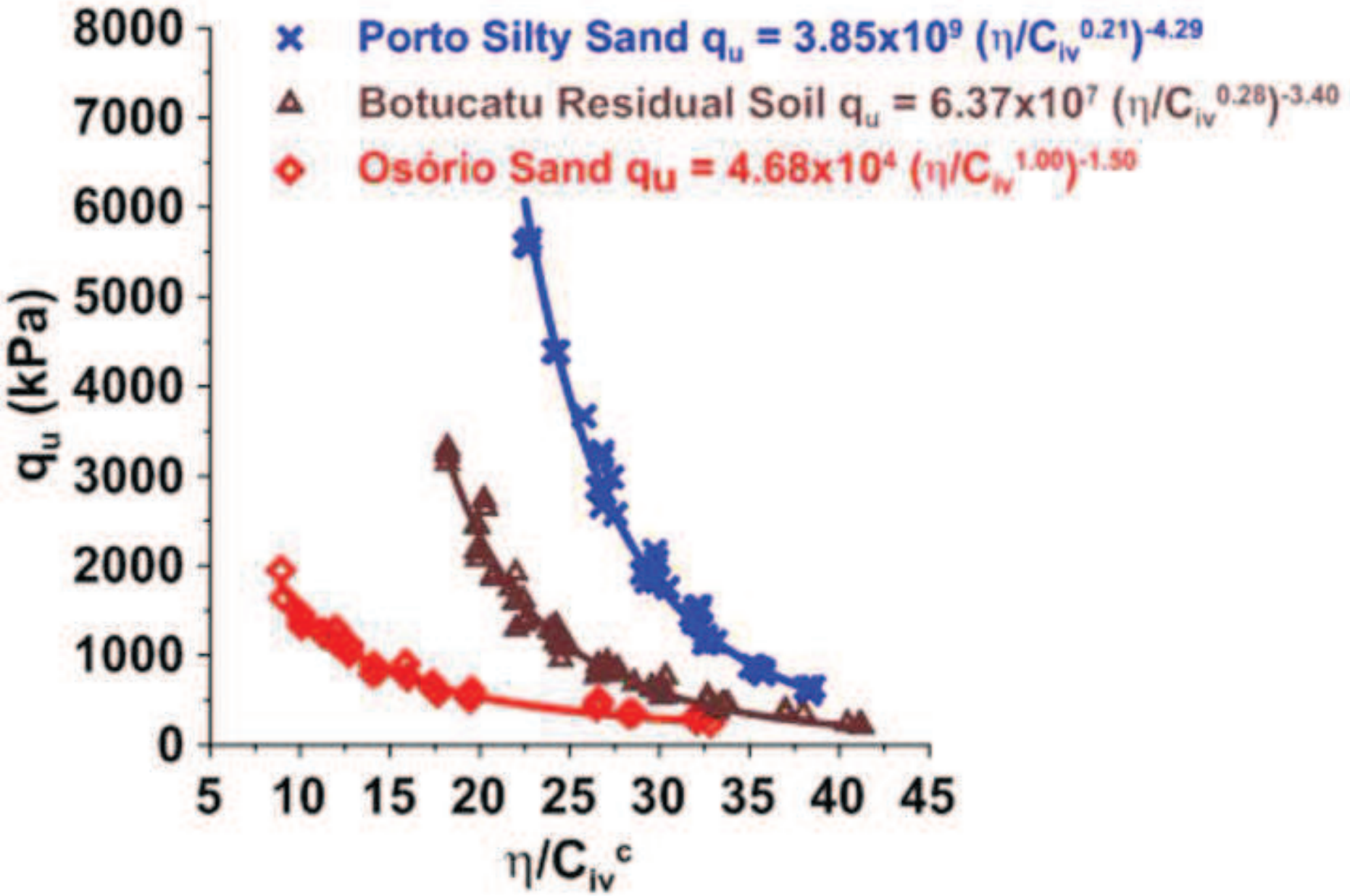

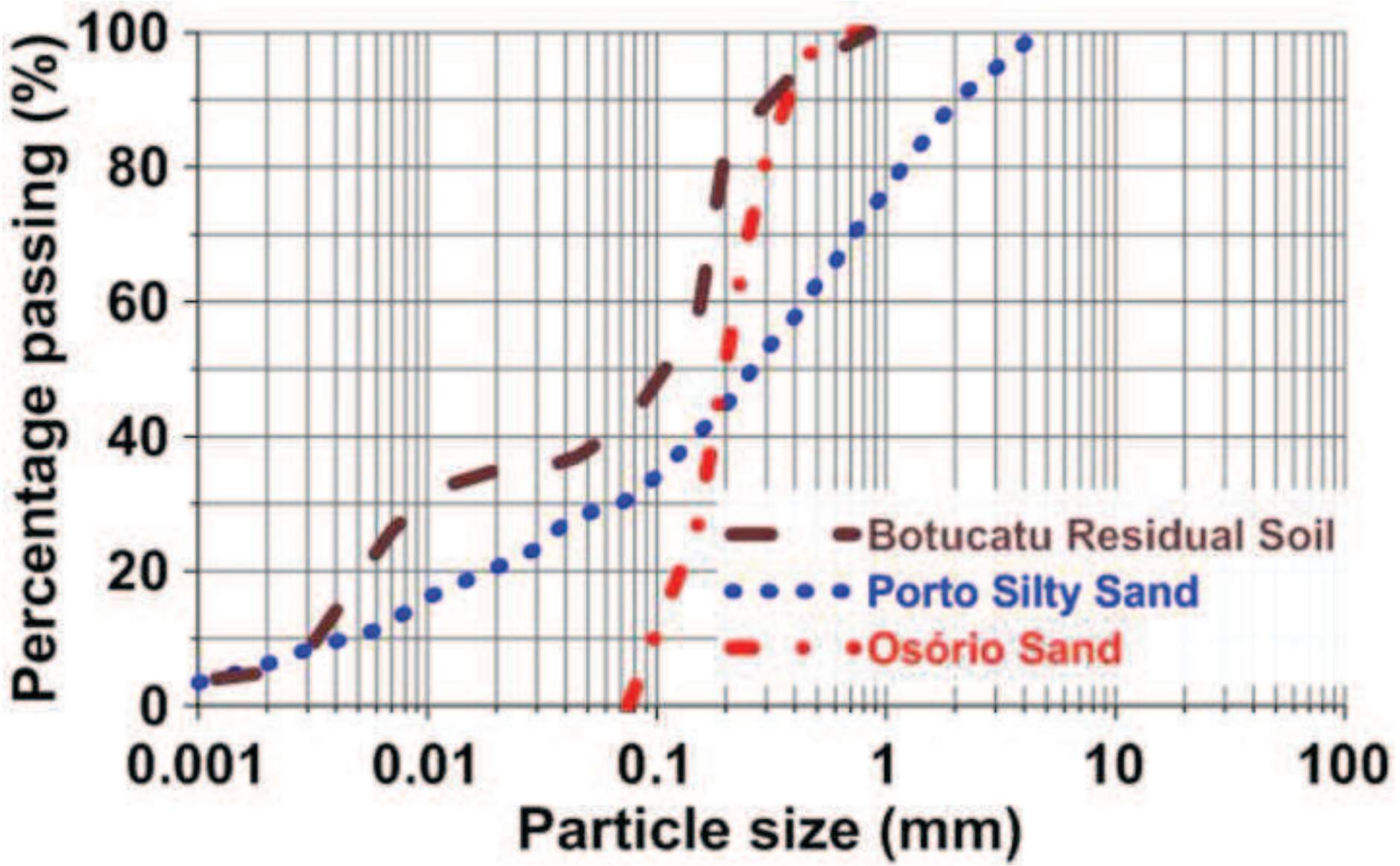

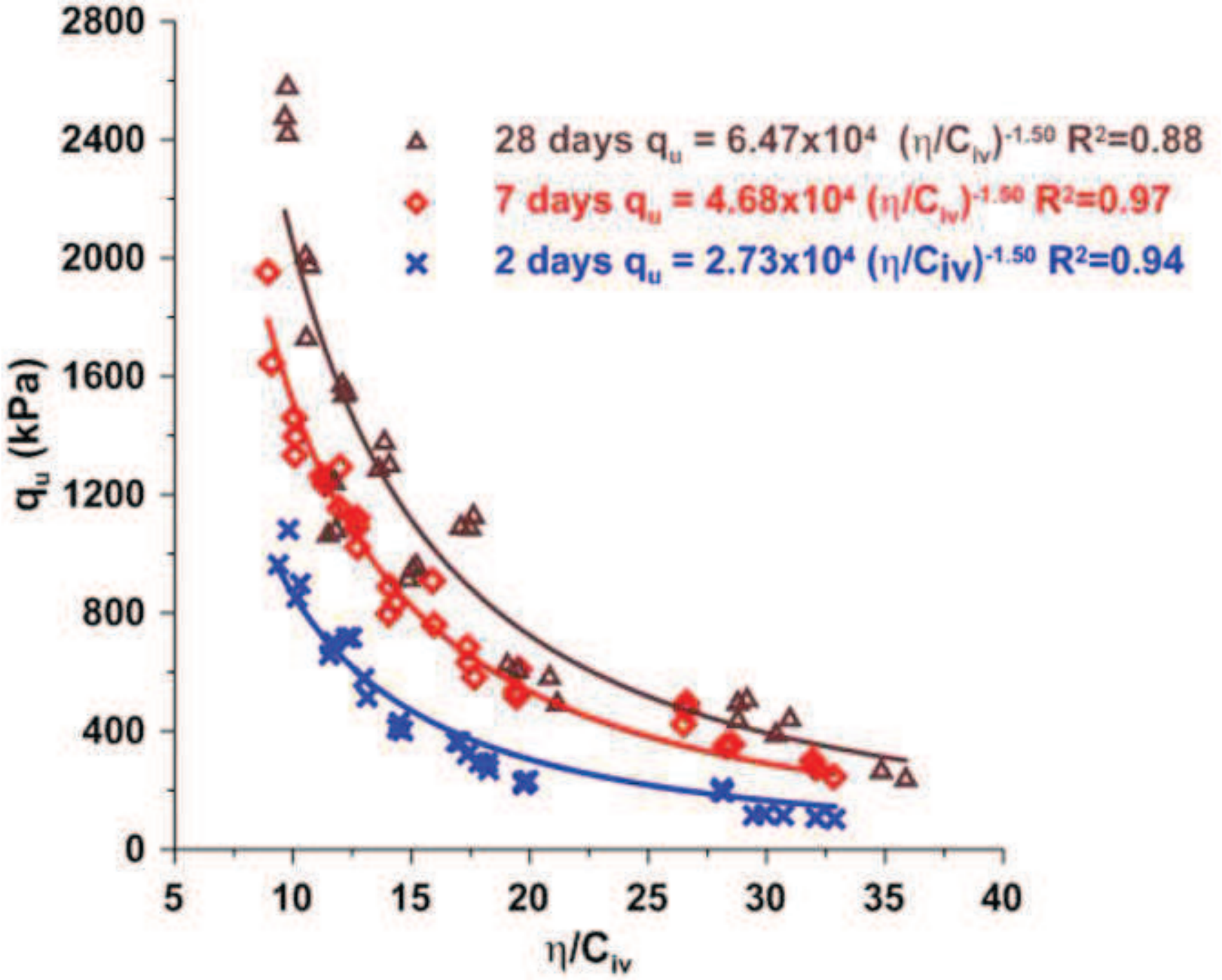

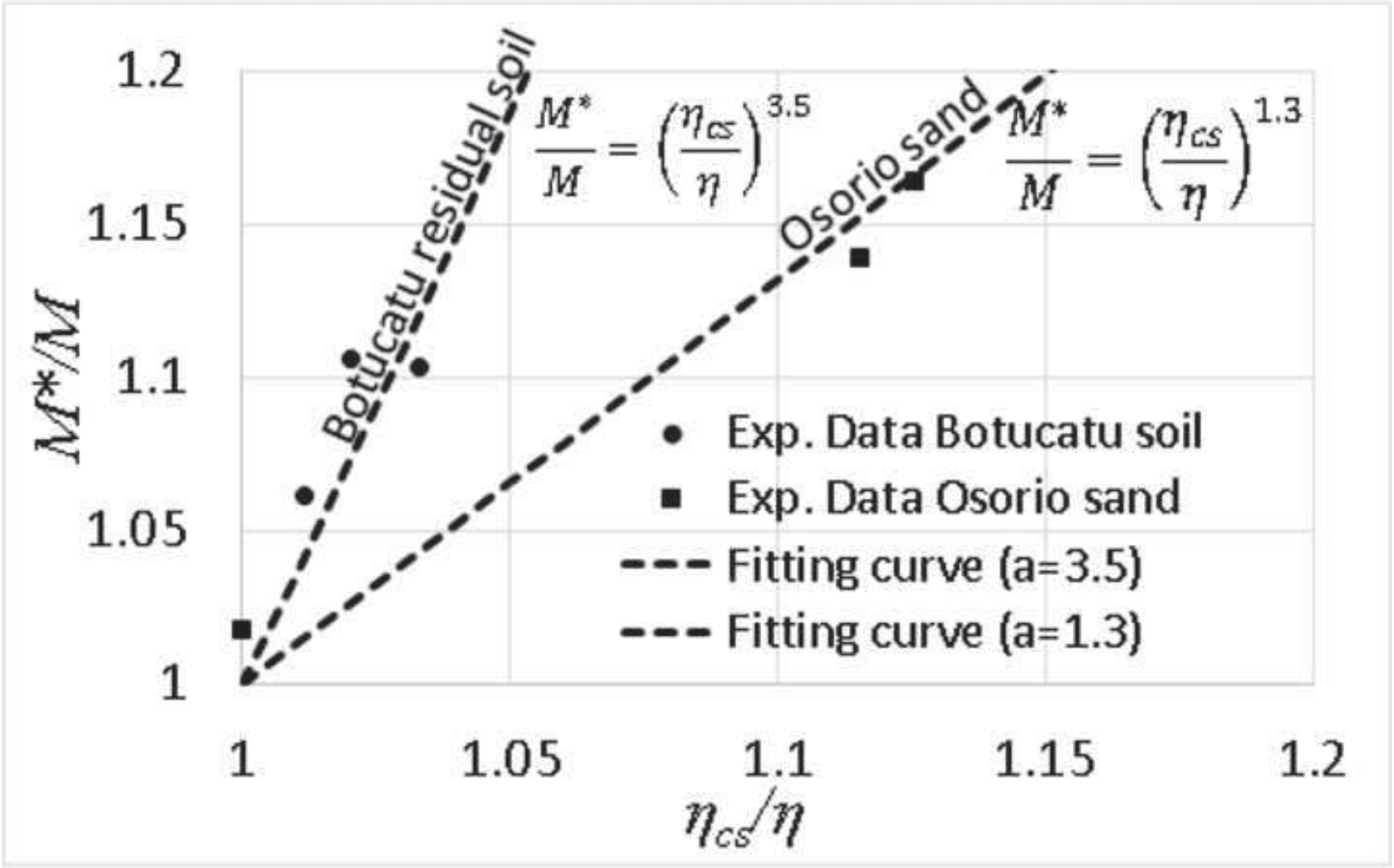

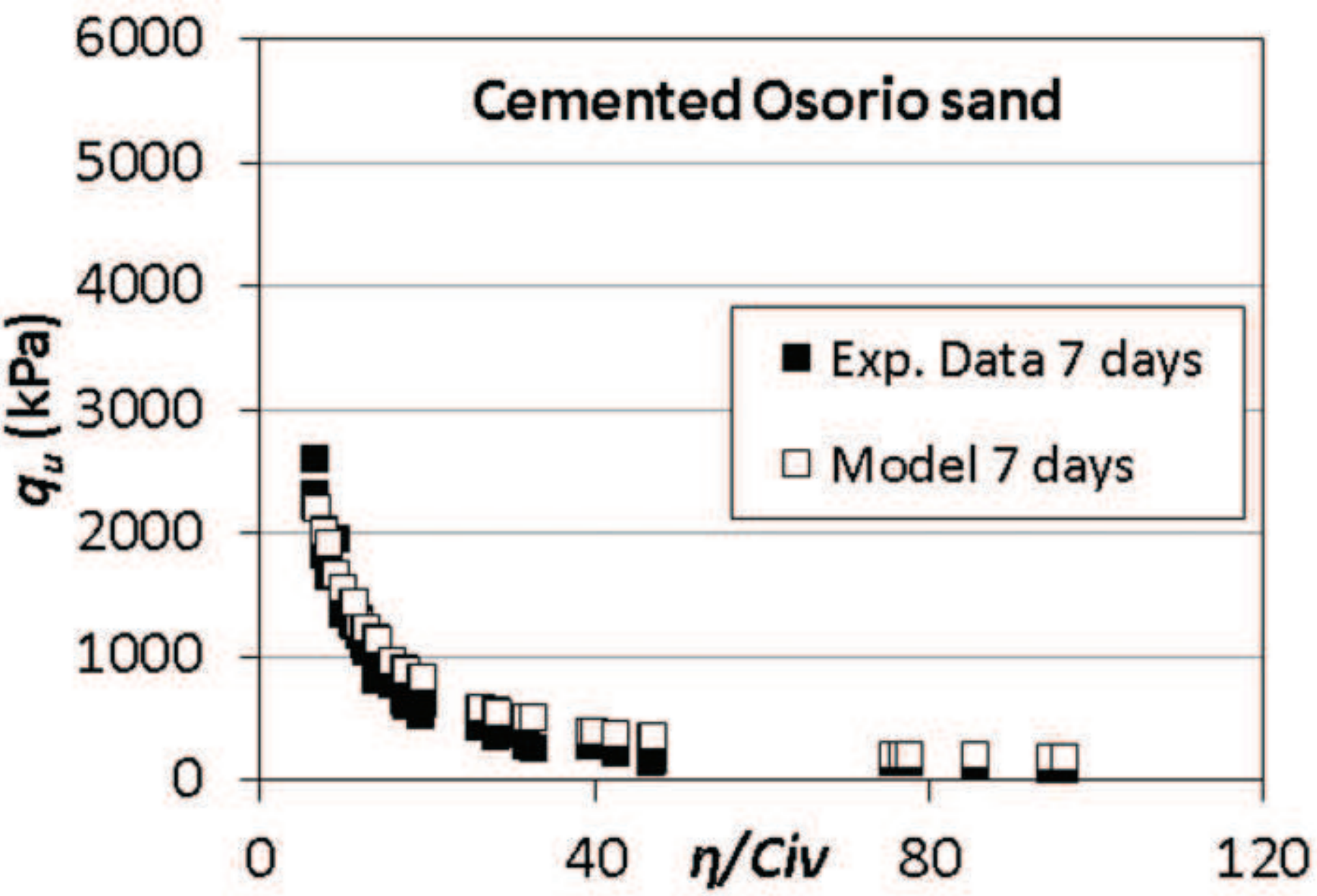

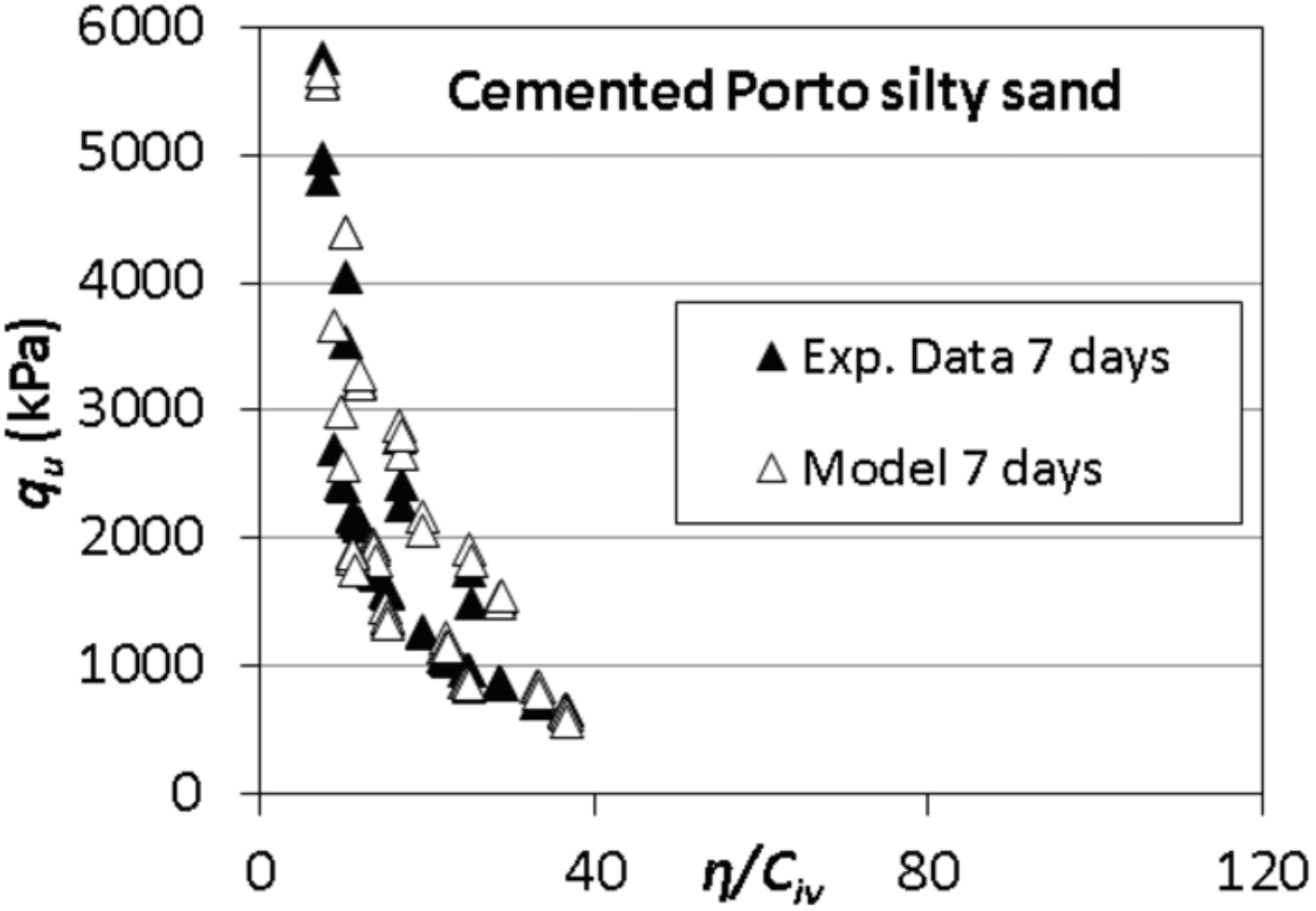

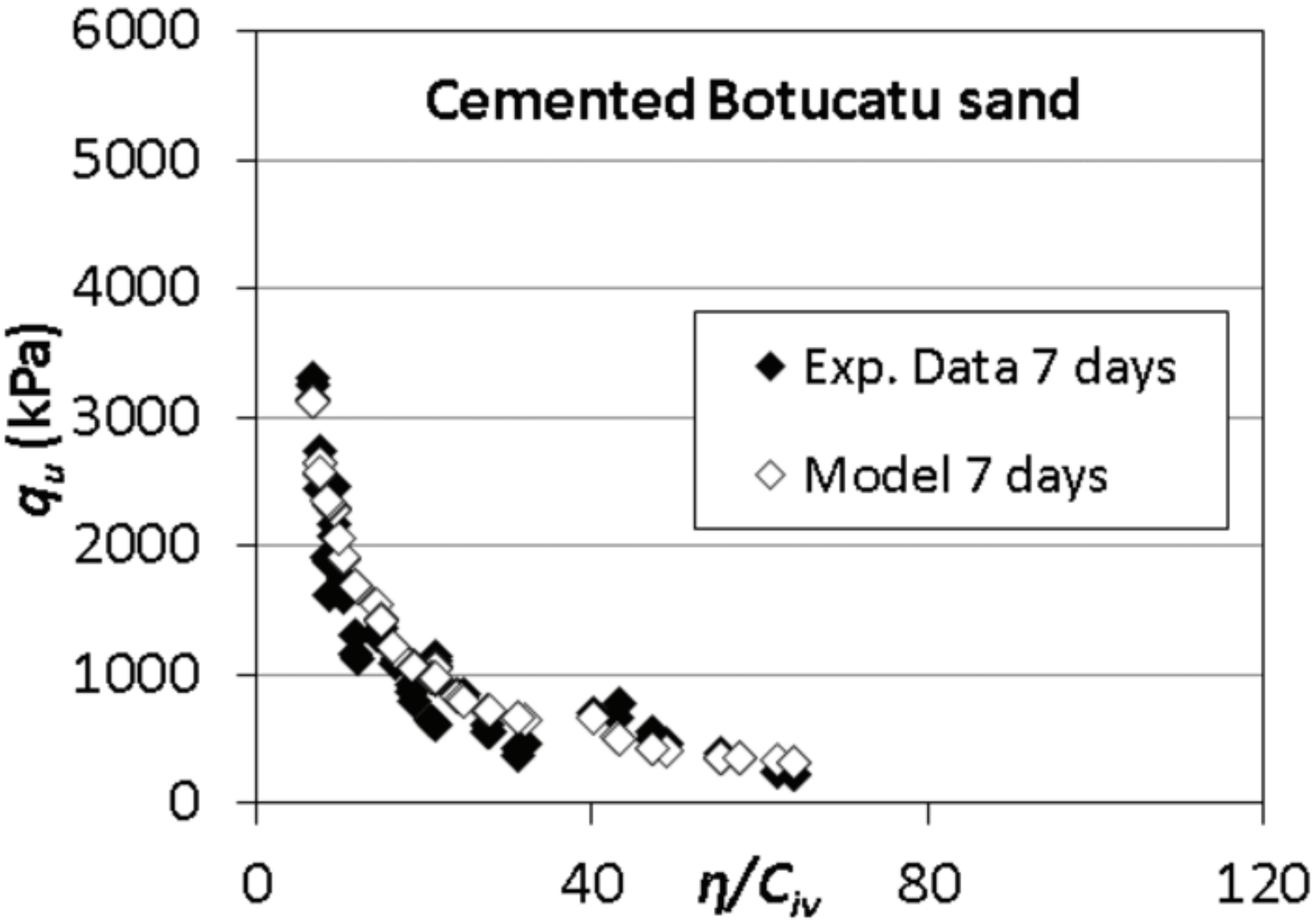

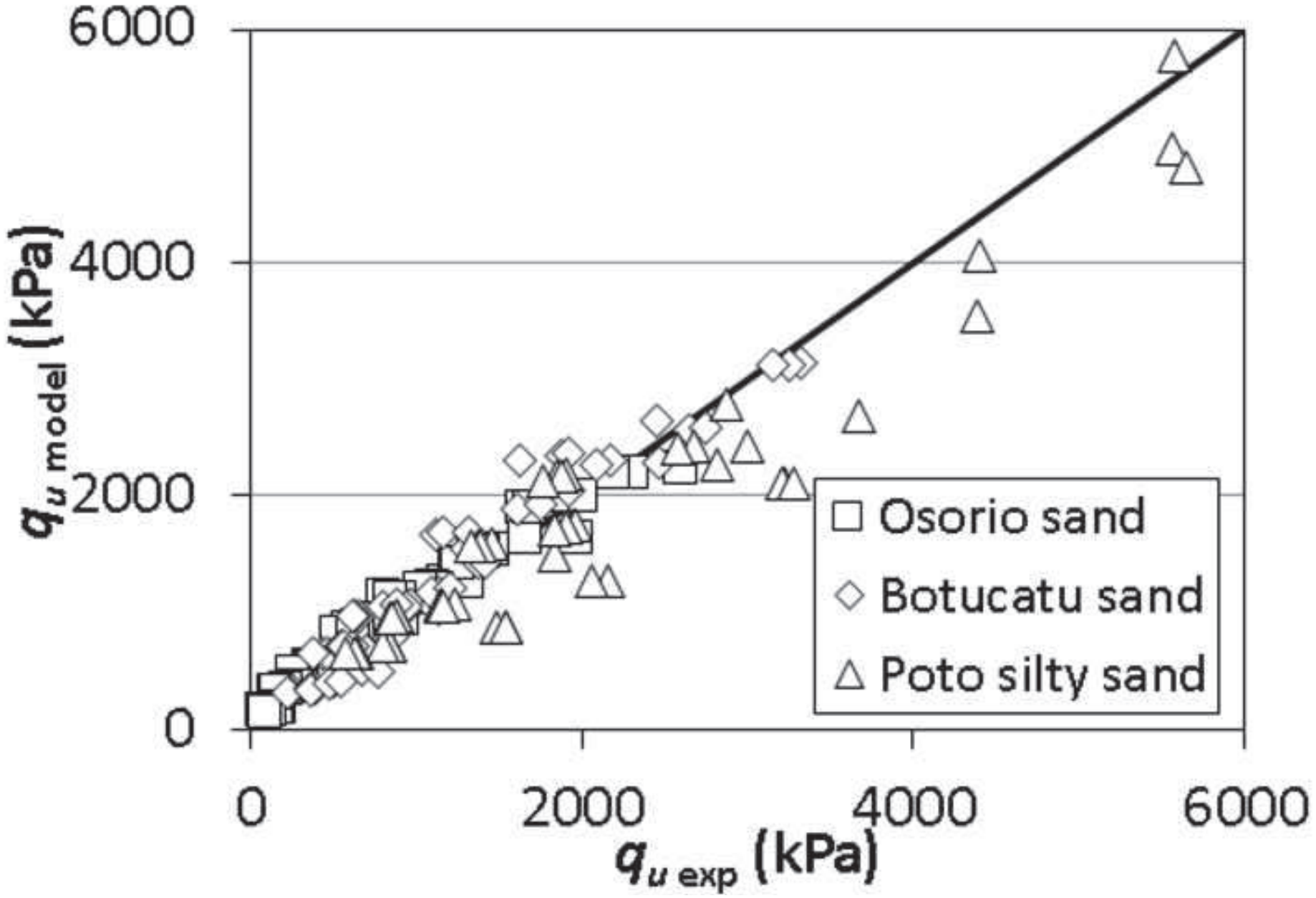

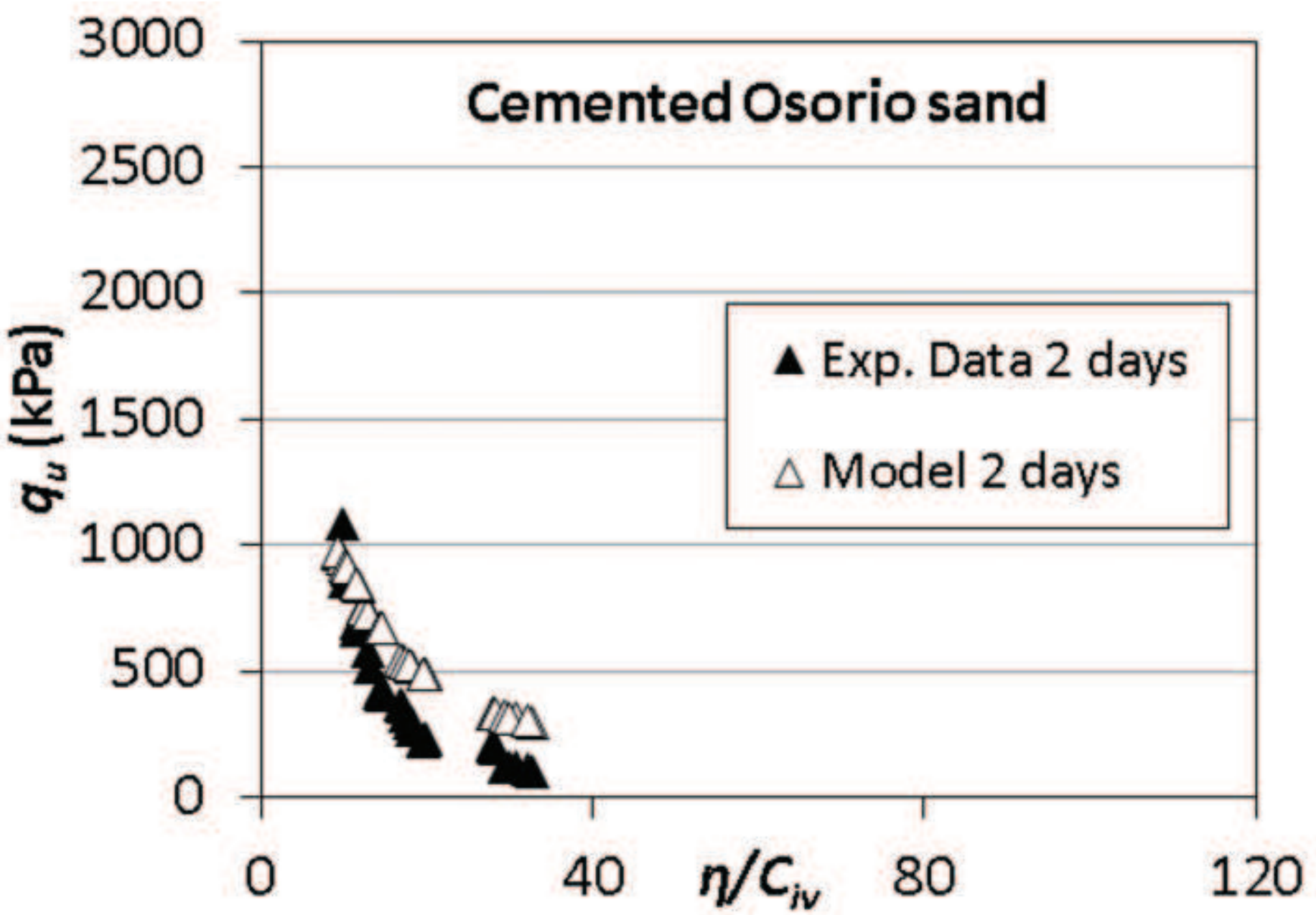

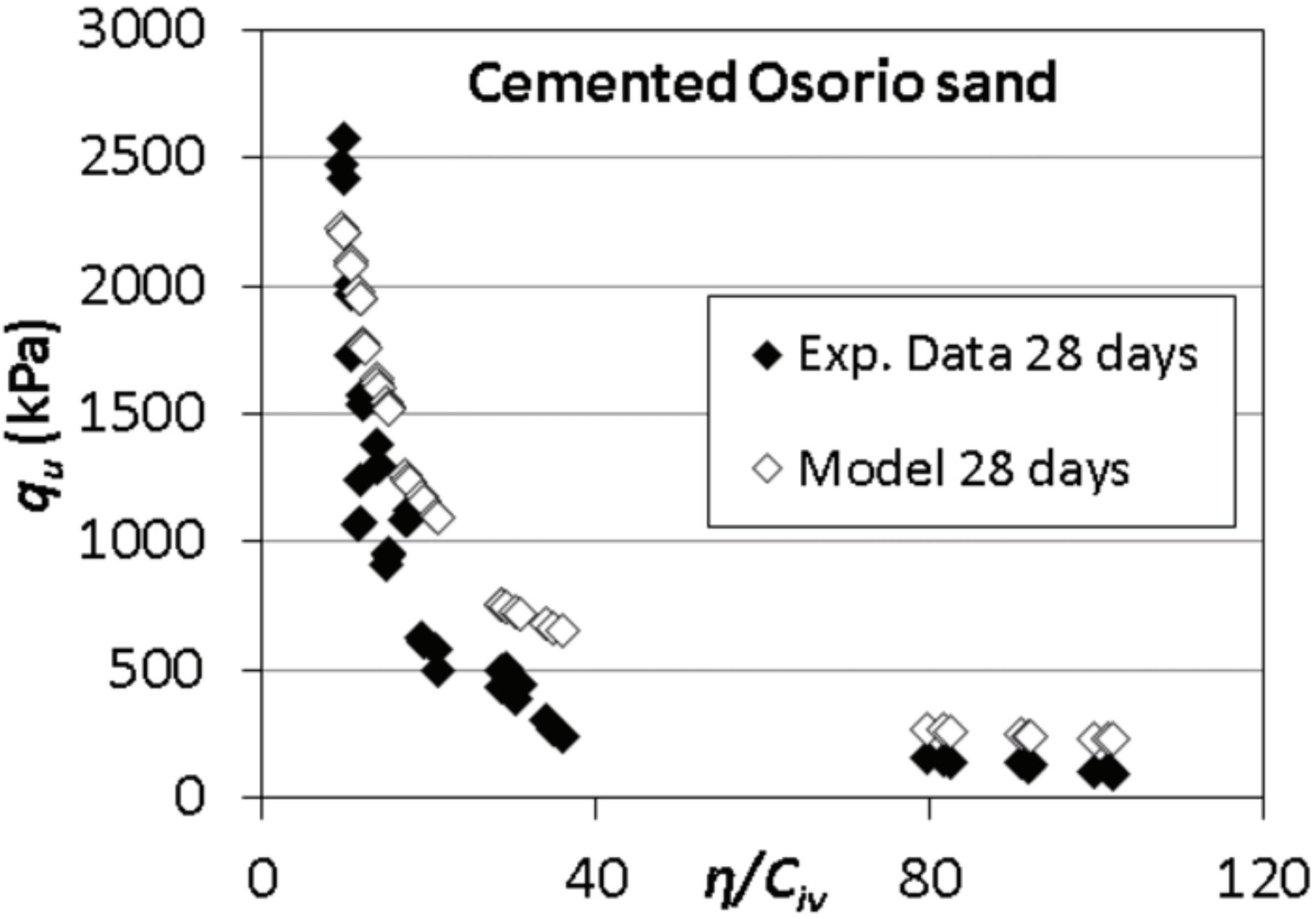

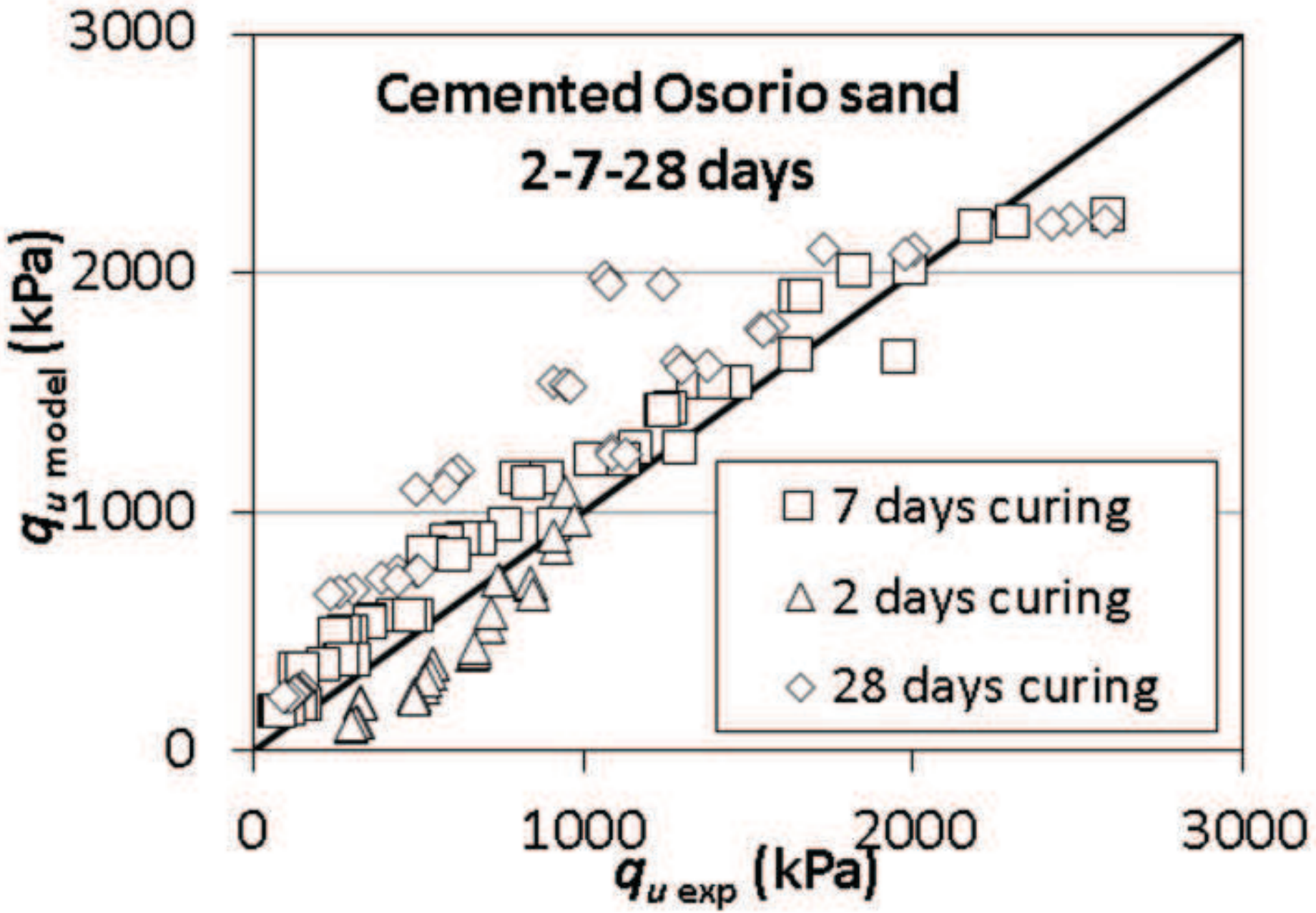

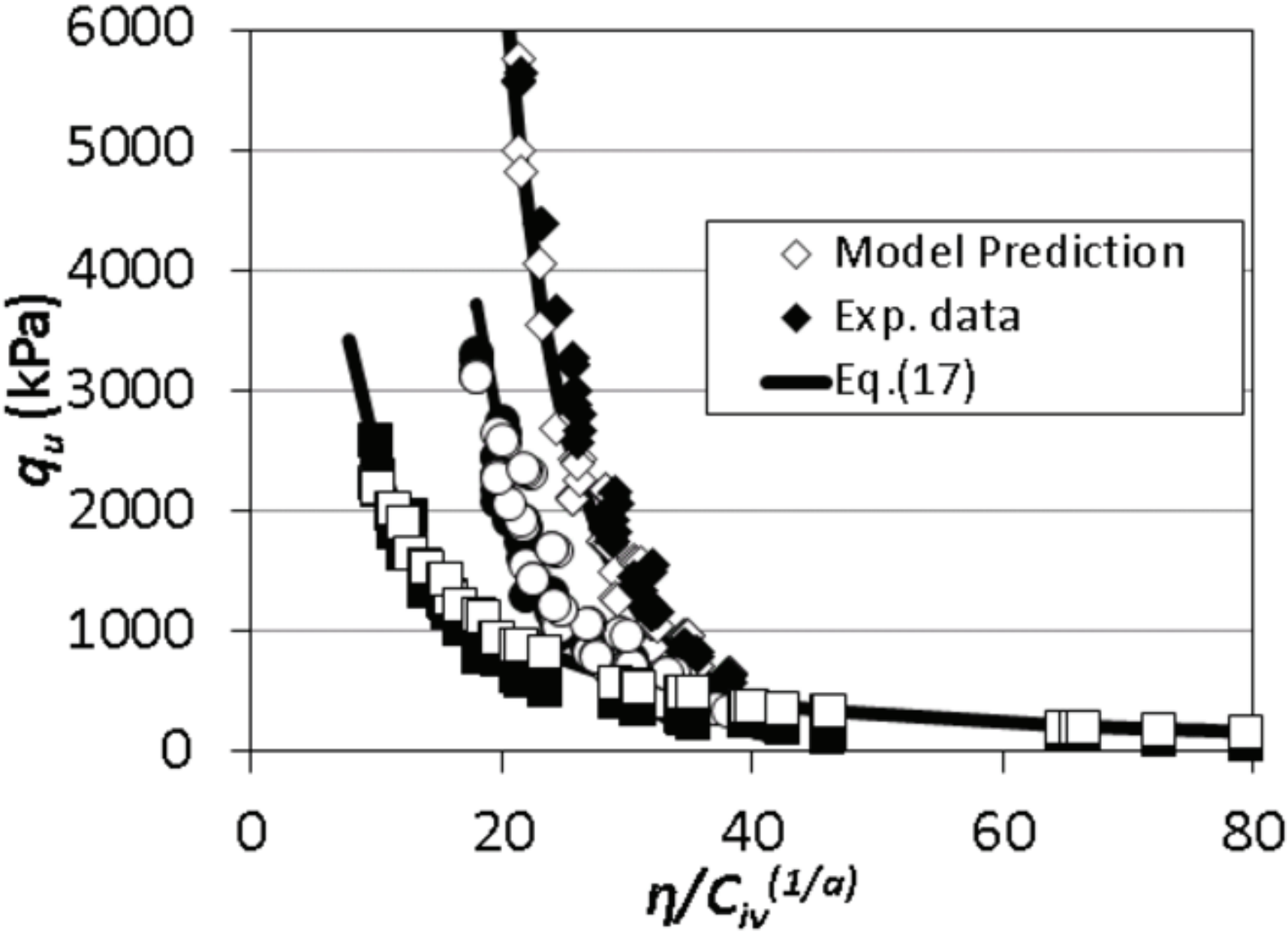

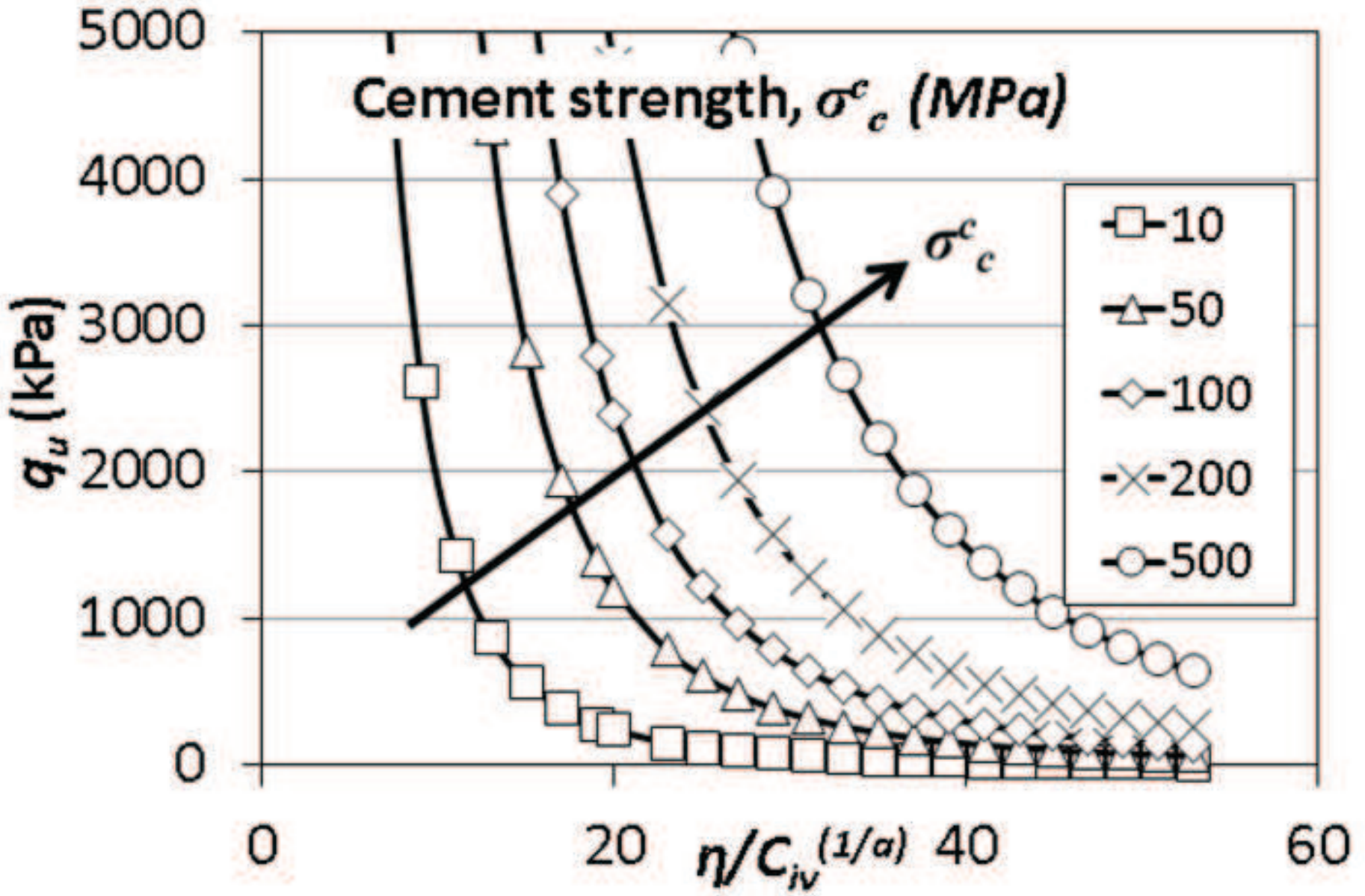

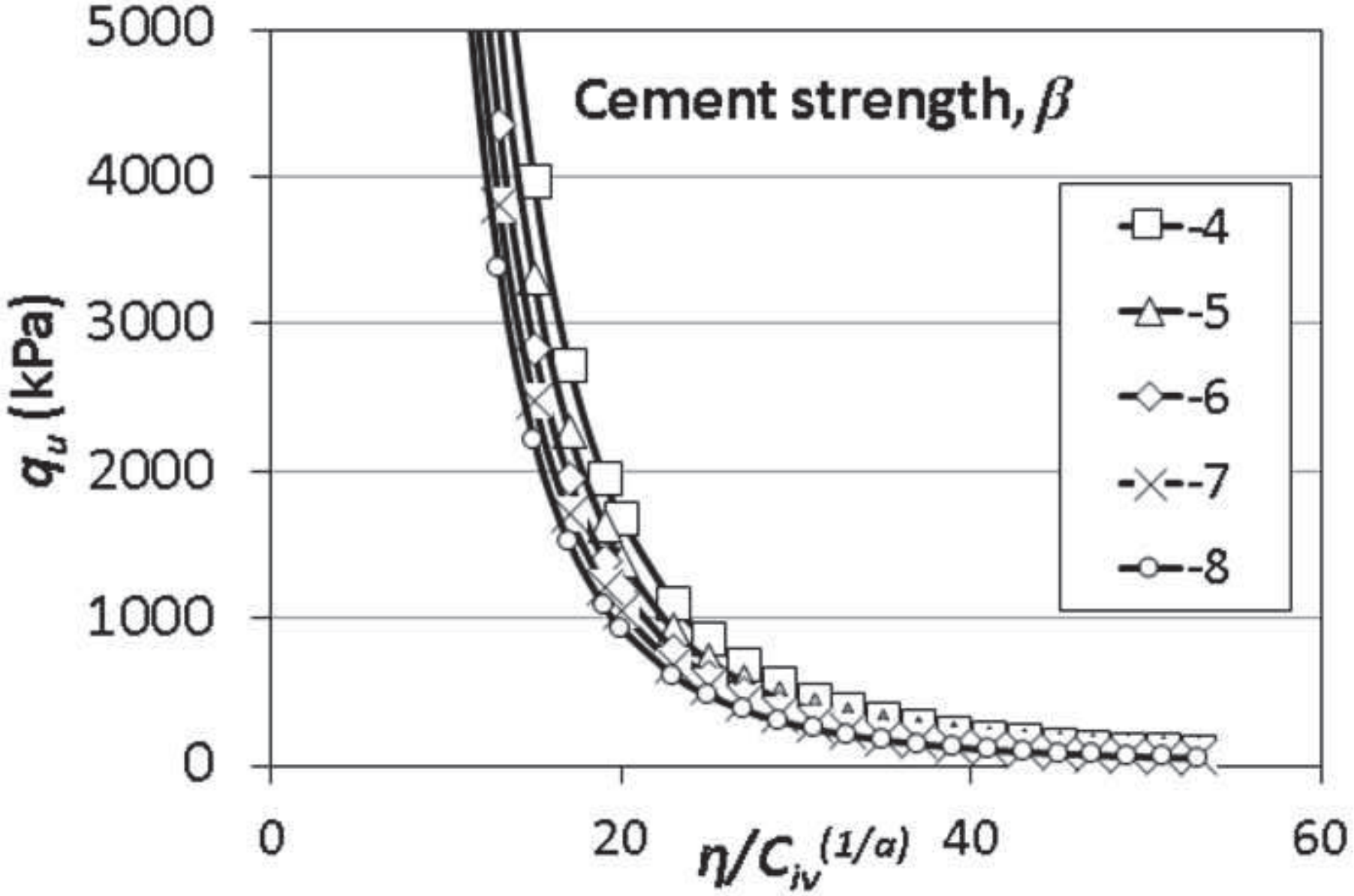

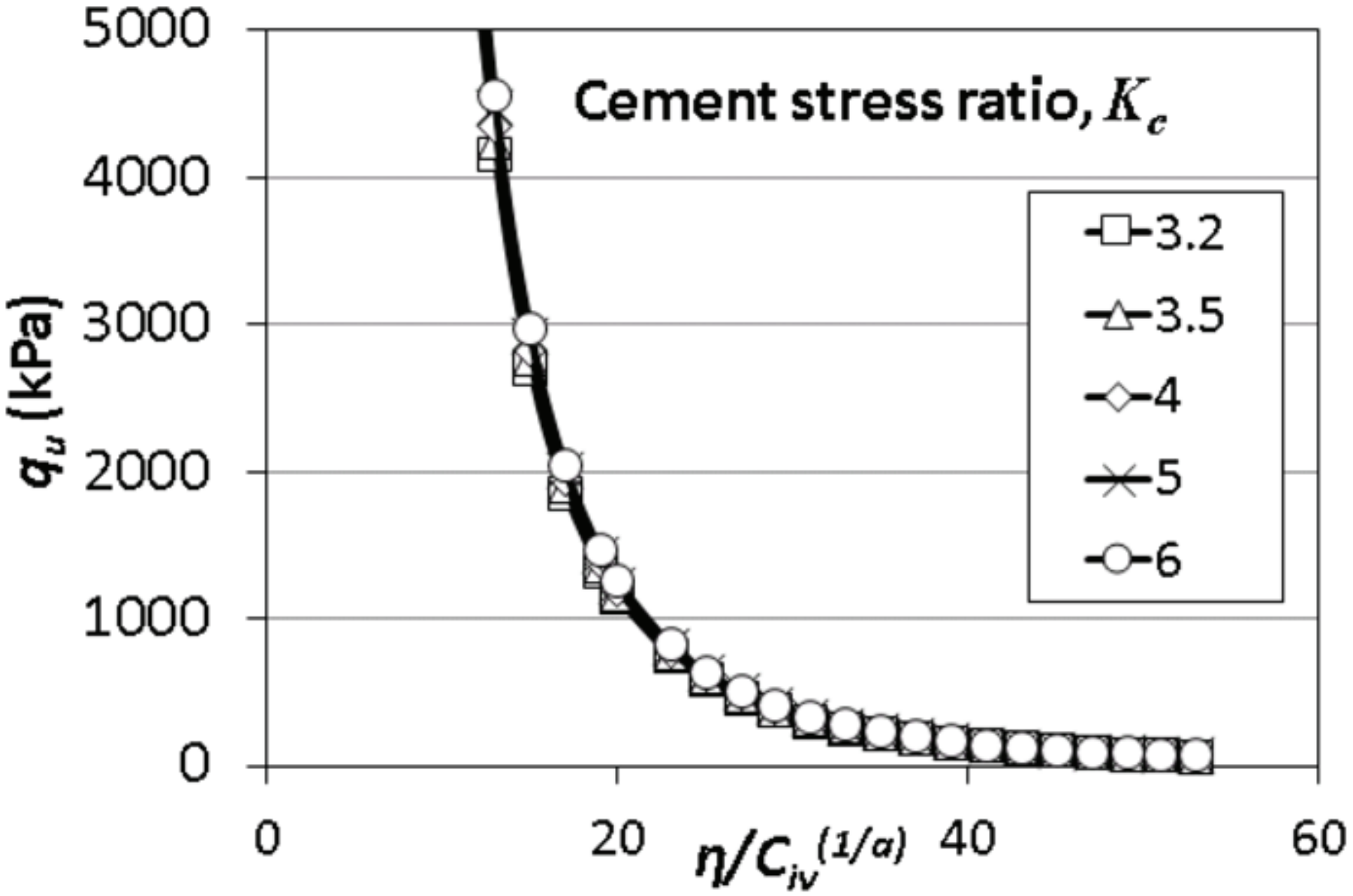

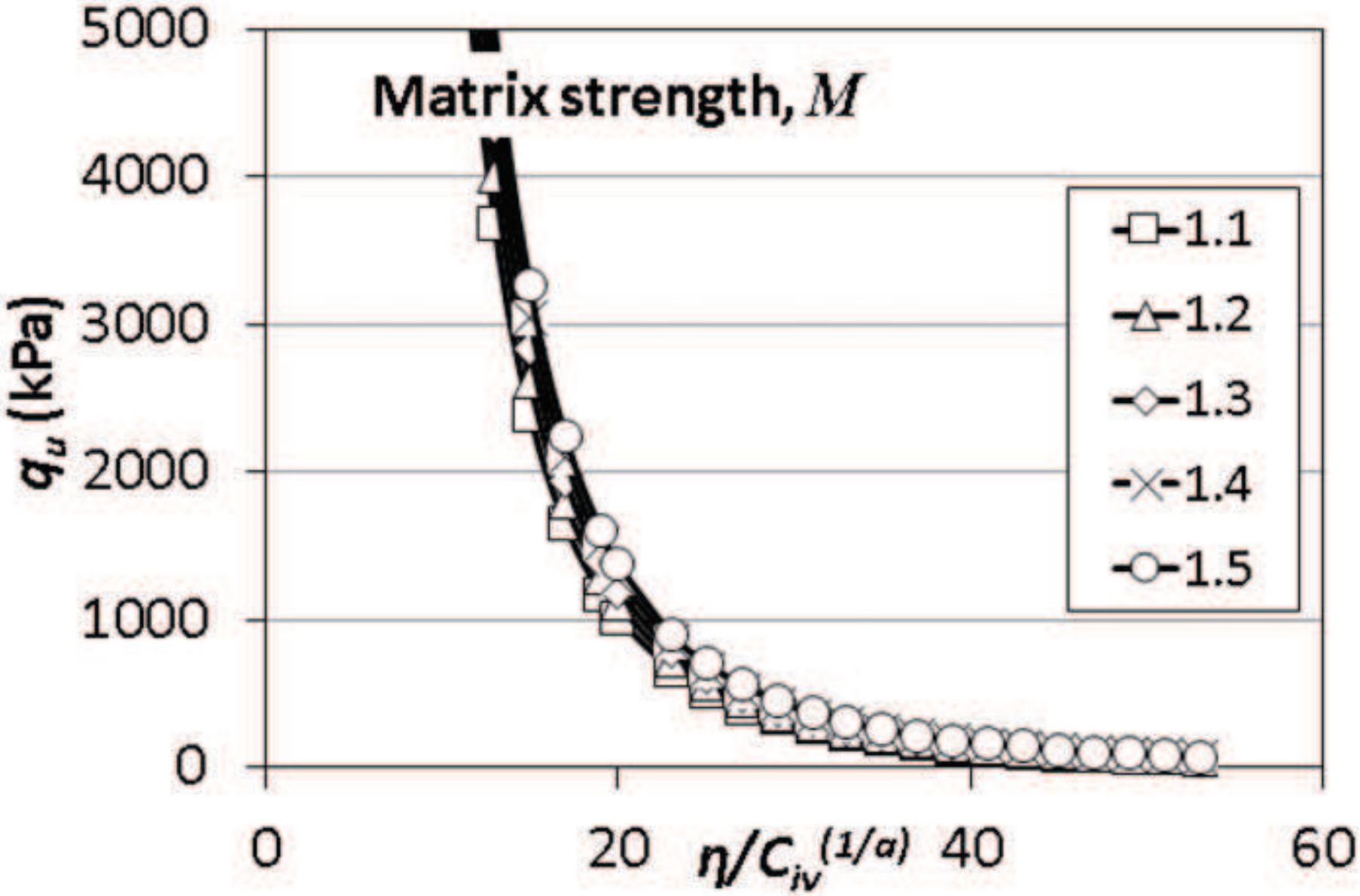

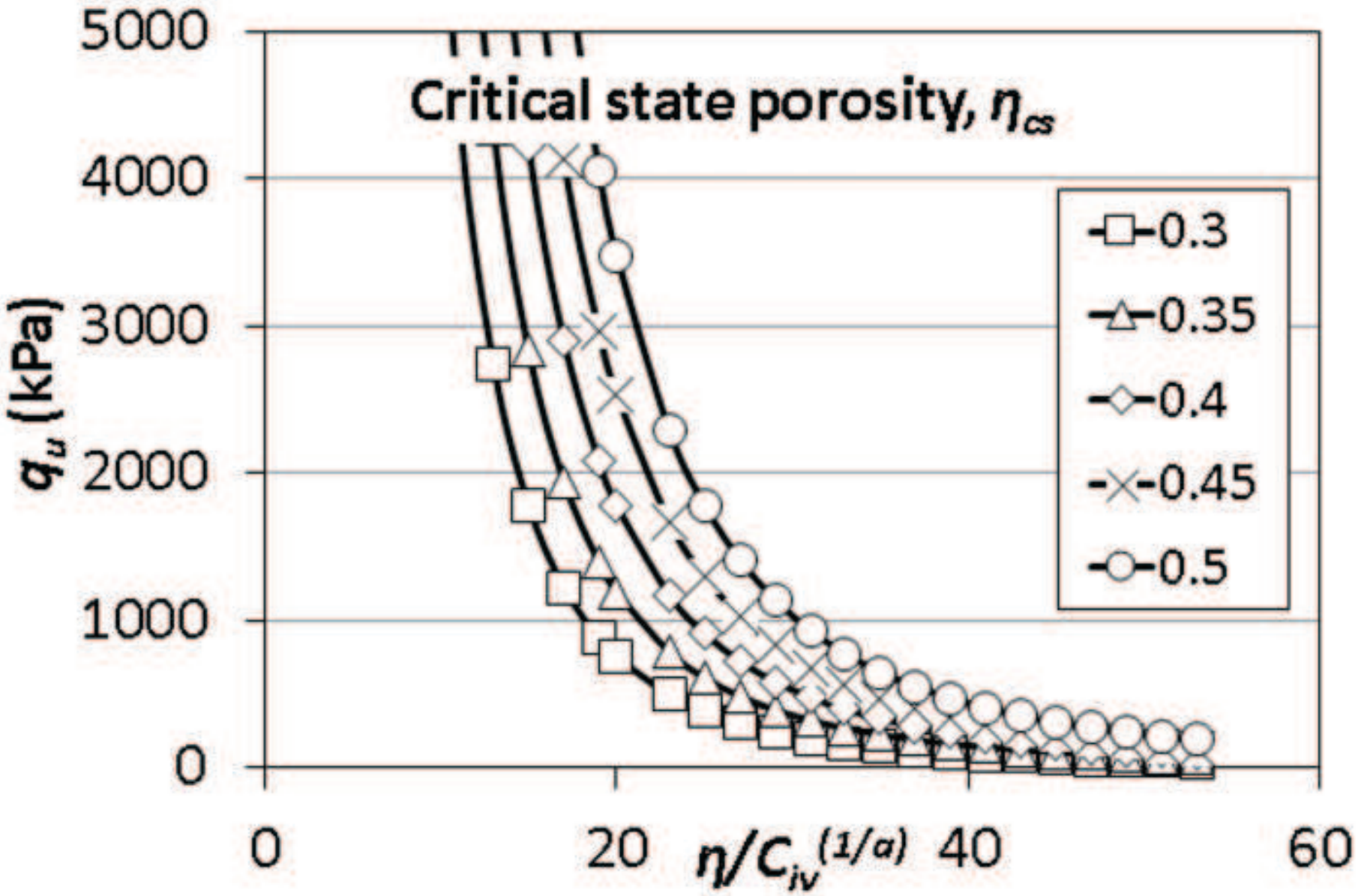

Figure

Click here to download Figure Fig7f_rev.tif

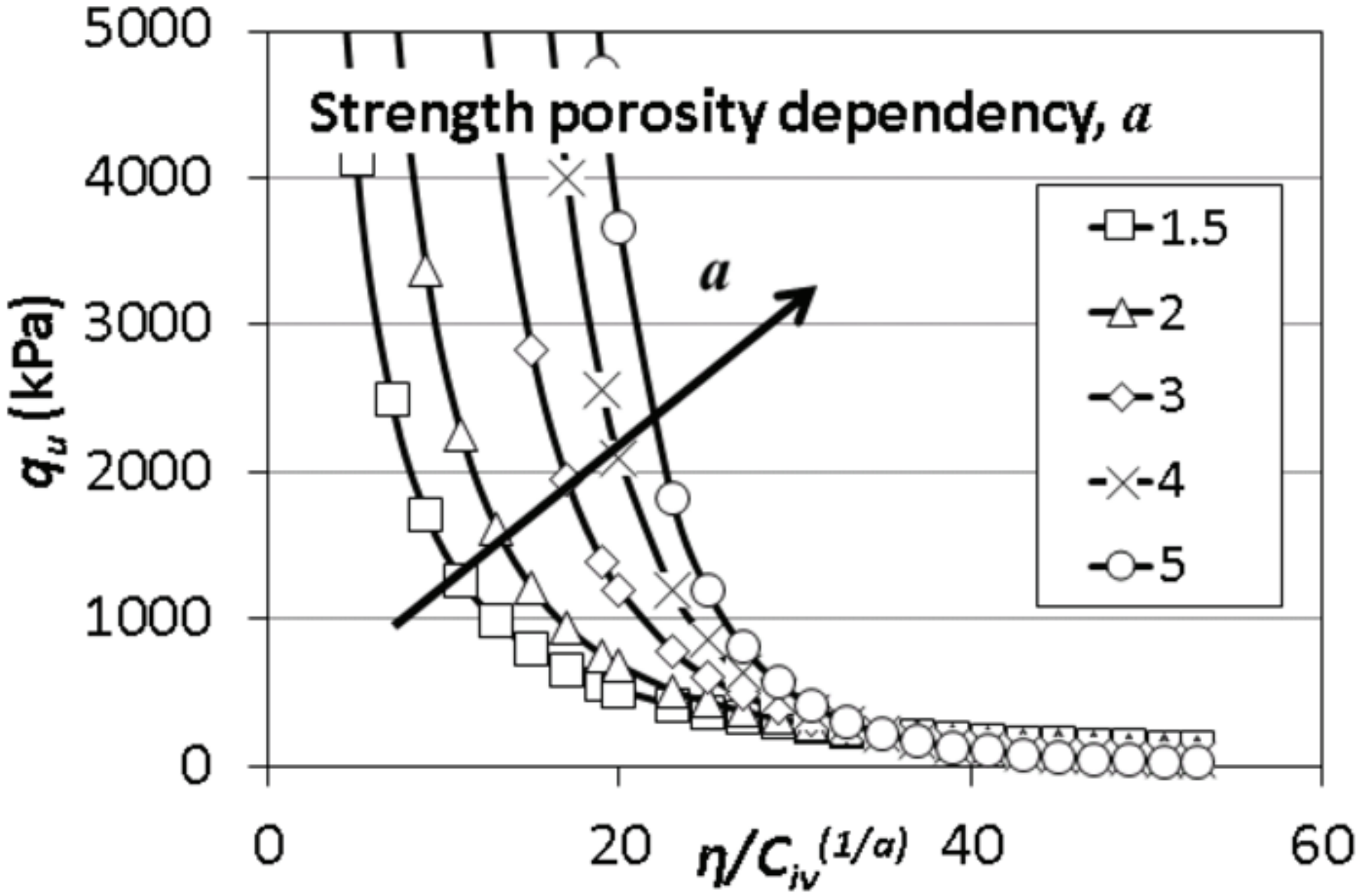

List of captions

Fig. 1. (a) Variation of unconfined compressive strength (q_u) with adjusted porosity/cement ratio for three soil types treated with early strength Portland cement (adapted from Consoli *et al.* 2007, 2012, 2013) after 7 days curing time; (b) particle size distribution of the sandy soils

Fig. 2. Variation of unconfined compressive strength (q_u) with adjusted porosity/cement ratio for Osorio sand treated with early strength Portland cement and cured for different lengths of time (adapted from Consoli *et al.* 2013).

Figure 3. Calibration of parameter a for Osorio sand and Botucatu residual soil using peak strength data from triaxial tests by Dos Santos et al. (2010) and Schnaid et al. (2001), respectively.

Figure 4. Comparison between model prediction and experimental results for three different types of cemented soils cured for 7 days: (a) Osorio sand, (b) Porto silty sand and (c) Botucatu residual soil. (d) reports a direct comparison between model predictions and experimental results for the three soils.

Figure 5. Comparison between model predictions and experimental results for cemented Osorio sand cured for: (a) 2 days and (b) 28 days. (c) reports a direct comparison between model predictions and experimental results for the three curing periods available for cemented Osorio sand.

Figure 6. Comparison between experimental data, theoretical prediction and approximated formula (17).

Figure 7. Influence of parameters related to the cement (a, b and c) and soil matrix phases (d,e, and f) on model predictions. Basic values of the soil parameters used in this exercise are: σ_c^c= 50 MPa, β=-6, K_c =4, M=1.3, η_{cs}=0.35 and a=3.